1214 Vol. 47, No. 5 / 1 March 2022 / Optics Letters Letter

Optics Letters

Real-time demonstration of 103.125-Gbps fiber–THz–fiber 2 × 2 MIMO transparent transmission at 360–430 GHz based on photonics

Jiao Zhang,[1,2] Min Zhu,[1,2,4] Mingzheng Lei,[2] Bingchang Hua,[2] Yuancheng Cai,[1,2] Yucong Zou,[2] Liang Tian,[2] Aijie Li,[2] Yanyi Wang,[3] Yongming Huang,[1,2] Jianjun Yu,[2,3] and Xiaohu You[1,2,5]

[1] National Mobile Communications Research Laboratory, Southeast University, Nanjing 210096, China
[2] Purple Mountain Laboratories, Nanjing, Jiangsu 211111, China
[3] Fudan University, Shanghai, 200433, China
[4] e-mail: minzhu@seu.edu.cn
[5] e-mail: xhyu@seu.edu.cn

Received 8 November 2021; revised 23 January 2022; accepted 25 January 2022; posted 25 January 2022; published 26 February 2022

In this Letter, we experimentally demonstrate the first real-time transparent fiber–THz–fiber 2 × 2 multiple-input multiple-output (MIMO) transmission system with a record line rate of 125.516 Gbps at 360–430 GHz based on photonic remote heterodyning, hybrid optoelectronic down-conversion, and commercial digital coherent modules. The 103.125-Gbps net data rate using dual-polarization quadrature phase-shift keying (DP-QPSK) modulation is successfully transmitted over two spans of 20-km standard single-mode fiber (SSMF) and 60-cm wireless distance under 15% soft-decision forward error correction (SD-FEC) for a pre-FEC bit error ratio (BER) threshold of 1.56×10^{-2} (post-FEC BER < 10^{-15}). The optical signal to noise ratio (OSNR) margin and the stability of the transmission system are extensively investigated. To the best of our knowledge, this is the first time to realize >100-Gbps real-time transparent fiber–THz–fiber link transmission at beyond the 350-GHz band, making it a promising scheme to pave the way towards a practical seamless integration of a fiber–THz–fiber link to the future 6G mobile communication system.

https://doi.org/10.1364/OL.448064

The explosive growth of wireless devices and bandwidth-consuming services, e.g., telemedicine, online courses, online meetings, and online offices, have promoted the demand for ultra-high data rate wireless communications. By 2030, 6G wireless traffic is expected to rival or surpass wired services [1]. Terahertz wireless communication is recognized as the key component of the future 6G mobile communication system [1–3]. The terahertz band (THz band, i.e., 0.3 THz to 10 THz) is attracting extensive attention in the interdisciplinary fields of electronics and photonics, which can provide a data capacity of hundreds of Gbps or even Tbps due to its huge available bandwidth [4,5]. In accordance with the World Radio Communication Conference 2019 (WRC-19) decision, the 275–296 GHz, 306–313 GHz, 318–333 GHz, and 356–450 GHz spectral bands are released for land mobile and fixed service applications, with a total spectrum bandwidth of 137 GHz [6], as shown in Fig. 1(a). Photonics-aided THz-wave technologies can break the bottleneck of electronic devices and exhibit the superior characteristics of high frequency, large bandwidth, and low transmission loss. It facilitates seamless integration with high-speed optical fiber access networks, which is expected to become an extremely promising application prospect for 6G [7]. The fiber–THz–fiber transmission system integrates long-distance and large-capacity advantages derived from joint fiber-optics and THz wireless transmission link. As shown in Fig. 1(b), a prospective seamless integration of a fiber–THz–fiber link can be used for a 1-Tbps point-to-point scenario over 1–2-km wireless distance and a >100-Gbps backhaul mesh scenario over 100–500-m wireless distance [8].

In recent years, the generation, modulation, and detection of broadband millimeter-wave and THz-wave signals based on photonic technology have effectively promoted the seamless integration of wireless networks and optical fiber networks [9–12]. Extensive fiber–wireless integration transmission systems have been demonstrated at the Q-, V-, W-, or D-band based on offline digital signal processing (DSP) [13–15]. The transparent optical–THz–optical link providing line-rates up to 240 and 190 Gbps over distances from 5 to 115 m at 230 GHz is demonstrated using a plasmonic modulator with a low-noise built-in amplification [16,17]. The transparent fiber–radio–fiber bridge at 101 GHz is also demonstrated using optical modulator and direct photonic down-conversion, and 32-/64-quadrature amplitude modulation (QAM) orthogonal frequency division multiplexing (OFDM) and single-carrier (SC) signals with line rates of 71.4 and 57.5 Gbps are transmitted [18]. However, the above research works are all based on offline DSP. Because of the bandwidth, sampling rate, and accuracy limitations of high-speed digital-to-analog/analog-to-digital converters (DAC/ADC), it is difficult to achieve real-time sampling and processing for ultra-high-speed communication

0146-9592/22/051214-04 Journal

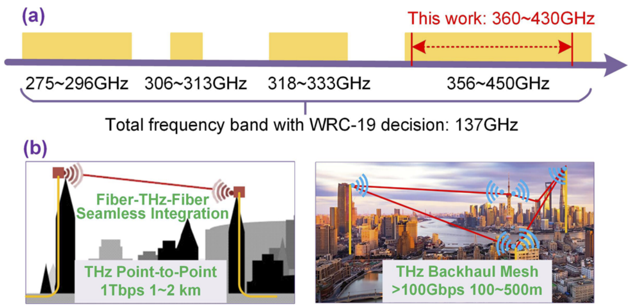

Fig. 1. (a) Spectrum release by the WRC-19 decision. (b) Prospective seamless integration of fiber–THz–fiber link scenarios.

data. By using high-speed real-time commercial digital coherent optics (DCO) modules, the transmission of 100-Gbps net capacity over two fiber links by a pure electronic THz wireless link at 300 GHz over 0.5-m wireless has been successfully demonstrated [19]. Also, the real-time delivery of 109.3-Gbps net data rate at 24 GHz based on a DCO module has experimentally been demonstrated [20]. Therefore, the commercial DCO module proves to be a promising solution to realize the practical seamless integration of a fiber–THz–fiber link. However, to the best of our knowledge, real-time >100-Gbps transparent fiber–THz–fiber transmission in the true sense at beyond the 350-GHz band based on photonics has not yet been reported.

In this work, we experimentally demonstrate a real-time photonics-aided transparent fiber–THz–fiber 2×2 multiple-input multiple-output (MIMO) transmission system based on photonics at up to the 360–430-GHz THz band. By using two commercial Centum form-factor pluggable (CFP2) DCO modules, the 31.379-GBaud (125.516 Gbps) dual-polarization quadrature phase-shift keying (DP-QPSK) signal providing 103.125-Gbps net capacity is successfully transmitted over two spans of 20-km standard single-mode fiber (SSMF) and 60-cm wireless distance under 15% soft-decision forward error correction (SD-FEC) for a pre-FEC BER of 1.56×10^{-2} (post-FEC BER $< 10^{-15}$). This is the first time to realize >100-Gbps real-time transparent fiber–THz–fiber link transmission in accordance with the WRC-19 releasing the 356–450-GHz THz band.

The experimental setup of our real-time transparent fiber–THz–fiber 2×2 MIMO transmission system is shown in Fig. 2. We built a 100-GbE (103.125 Gbps) transmission platform including two displayers, two servers, and two optical transport units (OTUs), between which four quad small form-factor pluggable 28 (QSFP28) modules are used on the client side, and two CFP2-DCO modules (InnoLight Technol., 200G CFP2 DCO MR) are equipped on the line side, as shown in Fig. 2(a). The parameters, including operating mode, wavelength, output optical power, pre-BER, and so on, can be set and monitored through the network management system (NMS) operation interface. The 100-GbE server network card is connected to the OTU through QSFP28 modules supporting 4×25.78125 Gbps over a 2-m multi-mode fiber (MMF). The CFP2-DCO module can support DP-QPSK modulation, polarization diversity homodyne detection, and high-speed real-time DSP demodulation. In our experiment, two CFP2-DCO modules work at the 100-GbE mode, and a 31.379-GBaud DP-QPSK modulated optical baseband signal with a roll-off factor of 0.2 is generated. The total bandwidth (BW) of the baseband signal is $31.379\times(1+0.2)=37.6548$ GHz. The CFP2-DCO module has a built-in optical transport network (OTN) framer and can be directly used for 100-GbE transponder application. The optical signal carrier frequency is 193.5 THz with 3-dBm output optical power. Then, the optical baseband modulation signal is delivered over one span of 20-km SSMF with an average loss of 0.2 dB/km and 17-ps/km/nm chromatic dispersion (CD) at 1550 nm.

At the fiber–THz wireless–fiber end, an erbium-doped fiber amplifier (EDFA) is used to compensate for the fiber transmission loss, and a passband tunable optical filter (TOF) is used to suppress the out-of-band amplified spontaneous emission (ASE) noise. A free-running tunable external cavity laser (ECL-1) is used as an optical local oscillator (LO), and has a linewidth of less than 100 kHz. The optical signal with 9-dBm optical power and ECL-1 with 12-dBm optical power are combined by an optical coupler (OC) and then amplified by an EDFA to effectively drive the antenna-integrated photomixer module (AIPM, IOD-PMAN-13001), which integrates a uni-traveling-carrier photodiode (UTC-PD) and a bow-tie or log-periodic antenna. A polarization beam splitter (PBS) is used to separate the X- and Y-polarization components of the combined lightwaves. In our demonstrated system, photonic heterodyning (up-conversion) is used to generate a THz-wave wireless signal with a tunable frequency range from 360 GHz to 430 GHz. Two parallel AIPMs, each with an operating frequency range from 0.3 THz to 2.5 THz and a typical −28-dBm output power, up-convert X- and Y-polarization components to two

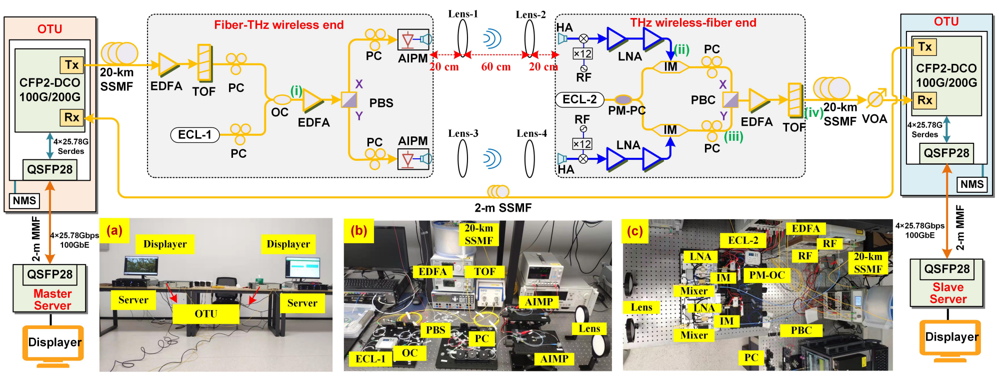

Fig. 2. Experimental setup of real-time photonics-aided transparent fiber–THz–fiber 2×2 MIMO transmission system over two spans of 20-km SSMF and 60-cm wireless distance. Photos of: (a) 100-GbE transmission platform; (b) fiber–THz wireless end; (c) THz wireless–fiber end.

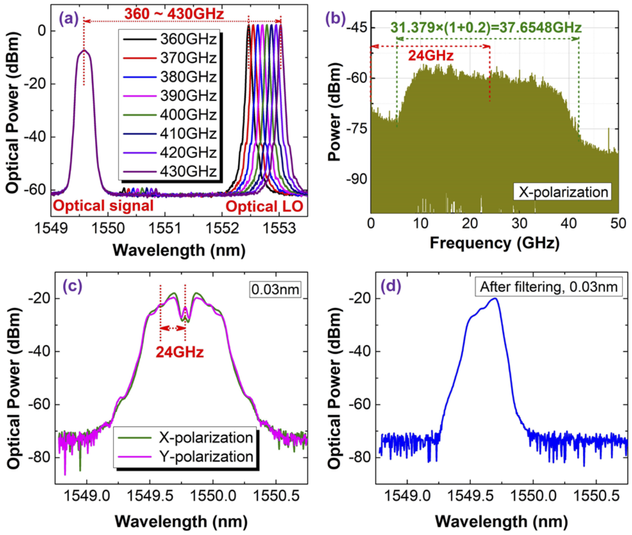

Fig. 3. Measured frequency spectrum after: (a) optical coupler; (b) low-noise amplifier; (c) intensity-modulator; (d) tunable optical filter.

THz-wave wireless signals. Note that the AIPMs are polarization sensitive, and hence four polarization controllers (PCs) are necessary to adjust the incident polarization direction to maximize output power from the AIPMs. Figure 2(b) shows a photo of the fiber–THz wireless end. After the PC, the measured optical spectrum for 360–430 GHz at 0.03-nm resolution is shown in Fig. 3(a). Then, the THz-wave signals are delivered over a 1-m 2×2 MIMO wireless THz-wave transmission link. Two pairs of lenses are used to focus the wireless THz-wave to maximize the received THz-wave signal power. The lenses 1–4 are identical, and each of them has a 20-cm focal length and 10-cm diameter. For an X-polarization (Y-polarization) THz wireless link, the separation distance between the AIPM and lens 1 (lens 3), lens 1 (lens 3) and lens 2 (lens 4), and lens 2 (lens 4) and the receiver horn antennas (HA) are 20 cm, 60 cm, and 20 cm, respectively.

At the THz wireless–fiber end, THz-wave wireless signals are received with two parallel THz-band HAs with 26-dBi gain. A photo of the THz wireless–fiber end is given by Fig. 2(c). For X- and Y-polarization THz-wave wireless signals, two identical THz receivers are driven by electronic LO sources to implement analog down-conversion, and each consists of a mixer, a ×12 frequency multiplier chain, and an amplifier, and operate between 330 GHz and 500 GHz. Then, the down-converted X- and Y-polarization intermediate-frequency (IF) signal at 24 GHz is boosted by two cascaded electrical low-noise amplifiers (LNAs) with a 3-dB bandwidth of 47 GHz to drive two intensity-modulators (IMs) each with a 3-dB bandwidth of 40 GHz. The electrical spectrum of X-polarization after LNAs is shown in Fig. 3(b). The ECL-2 as the optical carrier input of the two IMs, with 24-GHz frequency spacing to the initial optical baseband signal and 14.5-dBm optical power, is split by a polarization-maintaining OC (PM-OC) into two branches. Each IM is DC-biased at the optical-carrier suppression (OCS) point. Figure 3(c) shows the measured spectra after the IM in the case of the 370-GHz THz signal. Then, the X- and Y-polarizations are combined by a polarization beam combiner (PBC) and boosted by another EDFA. Two PCs are used to adjust the polarization direction to obtain the maximal output power. Another TOF is set to filter the upper sideband and the central optical carrier

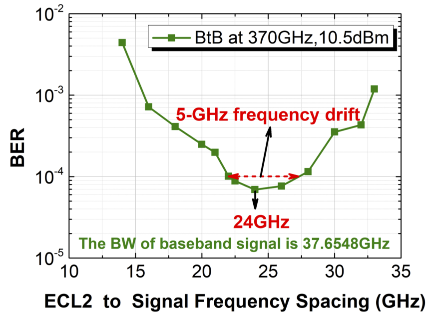

Fig. 4. BER versus ECL-2 to optical signal frequency spacing at 370 GHz with 10.5-dBm input power into each AIPM for the BtB case.

as well as the ASE noise, only leaving the lower sideband. Figure 3(d) gives the spectrum after the TOF. The obtained optical baseband signal is delivered over the second span of 20-km SSMF, and then received by the CFP2-DCO module. A variable optical attenuator (VOA) is used to measure the optical signal to noise ratio (OSNR) of the receiver. The symmetric reverse transmission path is directly connected via a 2-km SSMF.

We first measure the performance of our real-time transparent fiber–THz–fiber 2×2 MIMO transmission system for the back-to-back (BtB) case, i.e., without fiber and wireless distance transmission. The optical signal carrier frequency of the DCF2-DCO transmitter is constant operating at 193.5 THz. The center wavelength of ECL-1 is adjusted to generate the THz-wave wireless signals within the frequency range varying from 360 GHz to 430 GHz. Figure 4 gives the measured BER versus the ECL-2 to optical signal frequency spacing at 370 GHz with 10.5-dBm input power into each AIPM for the BtB case. We can find that there exists a 5-GHz frequency drift at the BER of 1×10^{-4}. When the frequency spacing between the optical baseband signal and ECL-2 is 24 GHz, the transmission system has the best BER performance. Based on the optimized device parameters, Fig. 5 shows the BER versus input power into each AIPM between 360 GHz and 430 GHz for the BtB case without fiber and wireless transmission. This digital coherent CFP2 module can support 15% SD-FEC for a pre-FEC BER of 1.56×10^{-2} (post-FEC BER $< 10^{-15}$). Therefore, the 31.379-GBaud (125.516 Gbps) DP-QPSK signal can provide 103.125-Gbit/s net capacity for a 100-GbE client. A THz-wave carrier frequency between 360 GHz and 430 GHz for the BtB case can be successfully real-time transmitted. The better BER performances occur at 370 GHz and 380 GHz. While the input power into each AIPM deviates from the best point at 11.5 dBm,

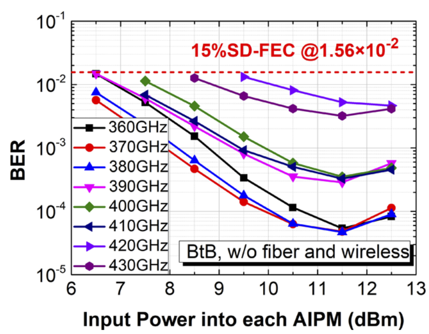

Fig. 5. BER versus input power into each AIPM for the BtB case without fiber and wireless transmission.

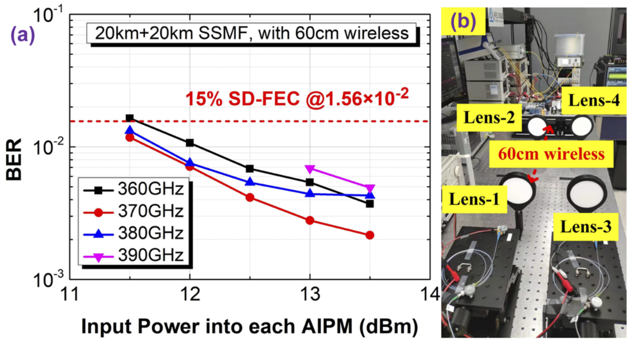

Fig. 6. (a) BER versus input power into each AIPM over two spans of 20-km SSMF and 60-cm wireless distance. (b) Photo of 1-m wireless link.

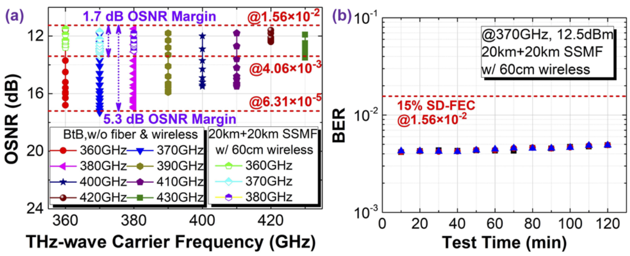

Fig. 7. (a) OSNR versus THz-wave carrier frequency for different cases. (b) BER versus test time at 370 GHz with 12.5-dBm input power into each AIPM over two spans of 20-km SSMF and 60-cm wireless distance.

the BER performance begins to deteriorate as the power of the AIPMs is saturated. There is an approximately 3-dB optical power penalty from 360 GHz to 430 GHz at the 15% SD-FEC threshold.

Then, we measure the BER versus the input power into each AIPM over two spans of 20-km SSMF and 60-cm wireless distance, as shown in Fig. 6(a). To protect the AIPMs, the maximum input optical power is set at 13.5 dBm. A THz-wave carrier frequency only between 360 GHz and 390 GHz can be successfully transmitted at the 15% SD-FEC threshold. The best BER performance occurs for the 370 GHz case. It may be because the AIPMs and THz receivers have a better frequency response at 370 GHz. Figure 6(b) shows a photo of the 60-cm wireless link. In Fig. 7(a), we also evaluate the OSNR of the receiver module for different cases of the THz-wave carrier frequency. The OSNR margin at 370 GHz for the BtB case and the two spans of 20-km SSMF and 60-cm wireless case is 5.3 dB and 1.7 dB, respectively. In the future, photonics combined with electronic active devices may leverage the THz wireless transmission distance for km-range.

Finally, we test the stability of the transmission system. We develop a streaming service platform based on EasyDarwin open-source software installed at the master server. Real-time video and live surveillance video are played successfully on the slave server as a user. Figure 7(b) gives the BER versus test time at 370 GHz with 12.5-dBm input power into each AIPM over two spans of 20-km SSMF and 60-cm wireless. This system can transmit stably within 120 minutes.

As a conclusion, in this Letter, a real-time transparent fiber–THz–fiber 2×2 MIMO transmission system with a record line rate of 125.516 Gbps and net data rate of 103.125 Gbps under 15% SD-FEC is experimentally demonstrated at 360–430 GHz based on photonic remote heterodyning, hybrid optoelectronic down-conversion, by virtue of the commercial CFP2-DCO module. To the best of our knowledge, this is the first time to realize >100-Gbps real-time transparent fiber–THz–fiber link transmission at beyond the 350-GHz band, making it a promising solution for the seamless integration of fiber–THz–fiber link applications.

Funding. National Natural Science Foundation of China (62101121, 62101126); China Postdoctoral Science Foundation (2021M702501); Transformation Program of Scientific and Technological Achievements of Jiangsu Province (BA2019026).

Disclosures. The authors declare no conflicts of interest.

Data availability. Data underlying the results presented in this paper are not publicly available at this time but may be obtained from the authors upon reasonable request.

REFERENCES

1. H. Elayan, O. Amin, B. Shihada, R. M. Shubair, and M.-S. Alouini, IEEE Open J. Commun. Soc. **1**, 1 (2020).
2. X. You, C.-X. Wang, and J. Huang, *et al.*, Sci. China Inf. Sci. **64**, 110301 (2021).
3. T. Nagatsuma, G. Ducournau, and C. C. Renaud, Nat. Photonics **10**, 371 (2016).
4. T. Harter, S. Ummethala, M. Blaicher, S. Muehlbrandt, S. Wolf, M. Weber, M. M. H. Adib, J. N. Kemal, M. Merboldt, F. Boes, S. Nellen, A. Tessmann, M. Walther, B. Globisch, T. Zwick, W. Freude, S. Randel, and C. Koos, Optica **6**, 1063 (2019).
5. H. Zhang, L. Zhang, S. Wang, Z. Lu, Z. Yang, S. Liu, M. Qiao, Y. He, X. Pang, X. Zhang, and X. Yu, J. Lightwave Technol. **39**, 5783 (2021).
6. L. Zhang, X. Pang, S. Jia, S. Wang, and X. Yu, *IEEE Commun. Mag.* **58**, 34 (2020).
7. Z. Chen, X. Ma, B. Zhang, Y. Zhang, Z. Niu, N. Kuang, W. Chen, L. Li, and S. Li, China Commun. **16**, 1 (2019).
8. T. Harter, C. Füllner, J. N. Kemal, S. Ummethala, J. L. Steinmann, M. Brosi, J. L. Hesler, E. Bründermann, A.-S. Müller, W. Freude, S. Randel, and C. Koos, Nat. Photonics **14**, 601 (2020).
9. T. Kawanishi, J. Lightwave Technol. **37**, 1671 (2019).
10. X. Li, J. Yu, and G.-K. Chang, J. Lightwave Technol. **38**, 366 (2020).
11. J. Yu, X. Li, and W. Zhou, APL Photonics **3**, 111101 (2018).
12. K. Sengupta, T. Nagatsuma, and D. M. Mittleman, Nat. Electron. **1**, 622 (2018).
13. J. Yu, IEEE J. Quantum Electron. **53**, 1 (2017).
14. X. Li, J. Yu, L. Zhao, K. Wang, C. Wang, M. Zhao, W. Zhou, and J. Xiao, J. Lightwave Technol. **37**, 196 (2019).
15. R. Puerta, J. Yu, X. Li, Y. Xu, J. J. Vegas Olmos, and I. Tafur Monroy, J. Lightwave Technol. **36**, 587 (2018).
16. S. Ummethala, T. Harter, K. Koehnle, Z. Li, S. Muehlbrandt, Y. Kutuvantavida, J. Kemal, P. Marin-Palomo, J. Schaefer, A. Tessmann, S. K. Garlapati, A. Bacher, L. Hahn, M. Walther, T. Zwick, S. Randel, W. Freude, and C. Koos, Nat. Photonics **13**, 519 (2019).
17. Y. Horst, T. Blatter, L. Kulmer, B. I. Bitachon, B. Baeuerle, M. Destraz, W. Heni, S. Koepfli, P. Habegger, M. Eppenberger, E. De Leo, C. Hoessbacher, D. L. Elder, S. Hammond, L. Johnson, Y. Fedoryshyn, Y. Salamin, M. Burla, and J. Leuthold, in *Optical Fiber Communication Conference (OFC)* (2021), paper F3C.1.
18. P. T. Dat, Y. Yamaguchi, K. Inagaki, M. Motoya, S. Oikawa, J. Ichikawa, A. Kanno, N. Yamamoto, and T. Kawanishi, in *Optical Fiber Communication Conference (OFC)* (2021), paper F3C.4.
19. C. Castro, R. Elschner, T. Merkle, C. Schubert, and R. Freund, in *Optical Fiber Communication Conference (OFC)* (2020), paper M4I.2.
20. C. Wang, X. Li, M. Zhao, K. Wang, J. Zhang, M. Kong, W. Zhou, J. Xiao, and J. Yu, in *Optical Fiber Communication Conference (OFC)* (2020), paper W2A.42.